

Article

Non-Linear Support Vector Machine Prediction of the Mechanical Properties of Asphalt Binders Subjected to Varying Temperatures and Frequencies Based on SARA

Shanglin Song ^{1,2}, Yiqian Ma ³, Xiaoqiang Jiang ⁴, Dengzhou Li ^{4,*}, Xiaoyan Ma ^{2,5,*} and Shidong Qiu ⁵¹ Gansu Provincial Highway Development Group Co., Ltd., Lanzhou 730070, China; 18193106299@163.com² Scientific Observation and Research Base of Transport Industry of Long Term Performance of Highway Infrastructure in Northwest Cold and Arid Regions, Lanzhou 736200, China³ The School of Surveying and Geoinformatics, Lanzhou Jiaotong University, Lanzhou 730070, China; 15506151339@163.com⁴ Gansu Hengtong Road and Bridge Engineering Co., Ltd., Lanzhou 730030, China; 13909380007@163.com⁵ Xi'an Key Laboratory of Modern Transportation Function Materials, Chang'an University, Xi'an 710064, China; 2021903592@chd.edu.cn

* Correspondence: lidengzhouyx@126.com (D.L.); xiaoyanma@chd.edu.cn (X.M.); Tel.: +86-15389401508 (X.M.)

Abstract: This study investigates the effects of chemical fractions on the mechanical properties of asphalt binders and predicts the mechanical properties of asphalt binders based on the chemical fractions. Initially, four fractions—saturate, aromatic, resin, and asphaltene (SARA)—were isolated from 36 asphalt binders using a thin-layer chromatography with flame ionization detection (TLC-FID) analyzer. Subsequently, the complex modulus and phase angle of the asphalt binders were determined for a range of frequencies and temperatures. The relationships between SARA content, heavy components, colloidal instability index, and the complex modulus and phase angle were analyzed. Advanced models, including quadratic polynomial and non-linear support vector machine (SVM) with sigmoid and RBF (Gaussian) kernels, were employed to predict the complex modulus and phase angle of asphalt binders based on the SARA data, and the reliability of these prediction models was critically assessed. The findings indicate that the contents of asphaltenes, resins, aromatics, and saturates significantly influence the rheological properties at different frequencies, though a clear correlation between SARA contents and both the complex modulus and phase angle was not established. Alternative methods should be considered for studying the mechanical properties of asphalt derived from SARA. The RBF kernel demonstrated superior performance compared to the quadratic polynomial and non-linear SVM with the Sigmoid kernel. While the non-linear SVM with the RBF kernel accurately predicts the complex modulus, it fails to predict the phase angle at low frequencies. The validation of this model confirmed its efficacy in capturing the relationship between input (SARA) and output (complex modulus and phase angle) vectors for each asphalt binder. The predicted complex modulus master curves closely match the experimental results, yet the model only approximates the trend of phase angle variation with frequency.

Keywords: mechanical properties of asphalt binders; SARA; non-linear SVM; prediction of complex modulus and phase angle master curves



Academic Editors: Valeria Vignali and Rafael Comesaña

Received: 22 October 2024

Revised: 17 December 2024

Accepted: 27 December 2024

Published: 8 January 2025

Citation: Song, S.; Ma, Y.; Jiang, X.; Li, D.; Ma, X.; Qiu, S. Non-Linear Support Vector Machine Prediction of the Mechanical Properties of Asphalt Binders Subjected to Varying Temperatures and Frequencies Based on SARA. *Coatings* **2025**, *15*, 62.

<https://doi.org/10.3390/coatings15010062>

Copyright: © 2025 by the authors.

Licensee MDPI, Basel, Switzerland.

This article is an open access article distributed under the terms and conditions of the Creative Commons Attribution (CC BY) license

(<https://creativecommons.org/licenses/by/4.0/>).

1. Introduction

As a by-product of the oil industry, bitumen is primarily used in building waterproofing, road pavement, and water resource dams. The performance and durability of these

structures are significantly influenced by the properties of bitumen, particularly in road paving. The characteristics of bitumen depend on the source of the crude oil and the manufacturing process, both of which contribute to variations in bitumen components. The saturates, aromatics resins, and asphaltenes (SARA) have a substantial impact on the rheological properties, stiffness, viscosity, aging, deformation, temperature sensitivity, and the degree of adhesion of bitumen to aggregates in the asphalt mixture [1]. The composition of bituminous components largely determines its performance, and any changes in composition directly result in changes to bitumen performance.

As the rheological indices of complex modulus and phase angle at various frequencies and temperatures determine the performance of bitumen, researchers have separated bitumen into saturates, aromatics, resins, and asphaltenes to study their mechanical properties. This separation helps further understand how composition influences the properties of asphalt. Regarding their specific properties, saturates and aromatics are oily liquids at room temperature, while resins are semi-solid, and asphaltenes are solid materials, resulting in distinct viscoelastic properties for these components. For saturates, the complex shear modulus exhibits an almost linear relationship with frequency reduction, while the phase angle remains constant at about 20° ; for aromatics, the complex shear modulus master curve resembles that of asphalt binders, and the phase angle curve levels off at 80° around 10 Hz. Resins display similar trends and glassy moduli as aromatics but reach the structure transition point at a lower frequency [2,3]. Xie's study reveals that saturates and aromatics show typical viscoelastic characteristics, contributing significantly to the flexibility of bitumen, with saturates displaying the lowest modulus at each frequency, although their phase angle varies widely. In contrast, resins exhibit the lowest phase angle but the highest modulus [4]. By segregating asphalt into four fractions and doping resins and asphaltenes into aromatics at varying contents to fabricate asphalt binders, researchers observed that increasing the content of resins or asphaltenes raises the complex shear modulus while lowering the phase angle value. Saturates maintain a constant phase angle regardless of temperature and frequency. Aromatics and resins share a similar Black diagram and master curve shape, characterized by a plateau in phase angle values [5]. The dynamic modulus shows a decreasing trend with increases in asphaltene or resin content and an increasing trend with increases in saturate or aromatic content [6–8]. By adding asphaltenes as a modifier, the stiffness, elasticity, and viscosity of bitumen increase, with every 6% addition of asphaltenes resulting in a one-interval rise in the high Performance Grade temperature grade [9].

Increasing asphaltene content also leads to a rise in the creep stiffness modulus and a decrease in the m -value at low temperatures, indicating that asphaltene content is a crucial determinant of the low-temperature flexibility of asphalt bitumen. Interestingly, however, the glass transition temperature (T_g) of asphalt binders is primarily influenced by the saturate and aromatic fractions, though it also increases with rising asphaltene content [10]. Kristina Hofer's research further confirmed that asphaltene content is inversely proportional to lower temperature performance [11]. Leite's studies on the lower temperature performance of asphalt binders revealed that hydrogen and carbon in the aromatic compounds are closely linked to binder stiffness; lower aromatic hydrogen content and higher saturated carbon content appear desirable for achieving lower stiffness at low temperatures [7]. Beyond macro-rheological properties, the micro-rheological properties of asphalt binders, characterized by the Derjaguin–Müller–Toporov (DMT) modulus, also increase with higher asphaltene and resin contents and decrease with higher saturate and aromatic contents. These micro-rheological results show good agreement with the macro-rheological properties [12]. Zhao's study indicated that changes in chemical properties leading to an increase in log dynamic viscosity depend on the type of binder and its age [13]. Studies using

molecular dynamics simulations to explore the initiation and cracking process of asphalt binders have shown that SARA influence the cracking process, with cracks appearing in areas with lower concentrations of asphaltenes and heteroatoms [14].

Salehfard examined 11 different asphalt binders, characterized by varying SARA compositions, to assess the impact of colloidal instability on rheological properties. The results indicated a notable increase in the viscosity of the asphalt binder corresponding to an increase in the I_c value. Additionally, there was a gradual shift of the Black curves towards higher complex moduli and lower phase angles, particularly at low frequencies, where the changes were significantly more pronounced than at high frequencies [15]. Further studies suggested that changes in the SARA analysis of bitumen serve as indicators of colloidal stability, with asphaltenes having a substantial impact. A higher asphaltene content resulted in less stability, leading to the asphalt binders being more gel-like [16].

Other research has focused on the internal colloidal structure of asphalt by examining the interactions among asphaltenes, resins, aromatics, and saturates. These studies revealed that resins and asphaltenes contain many unsaturated aromatic compounds and polar functional groups, making them more susceptible to aging than other fractions [17]. It was also found that the long-chain alkenes of saturates do not always reside on the outermost region of the colloidal structure; some penetrate the gaps within asphaltene molecules and adhere to the aliphatic areas [18]. Reconfiguring the internal colloidal structure of asphalt further demonstrated that as the distance from the center of the asphaltene micelle increases, polarity decreases. Oxidation predominantly occurs on the surface of the micelle mantles, with the highly polar aromatics and resins prone to oxidation, rendering the micelle mantles susceptible to aging [19].

Additionally, some researchers have focused on exploring the relationship between asphalt components and their safety in use, specifically the thermal properties of asphalt binders. By separating the SARA from the asphalt binder, their studies suggest that thermal stability increases progressively from saturates to asphaltenes [20]. When the heating rate is increased, the release of small molecular volatiles from saturates, aromatics, and asphaltenes increases, whereas the pattern is reversed for resins [21]. The thermal-oxidative aging of asphalt binder is characterized by endothermic reactions occurring in saturates and aromatics; both endothermic and exothermic reactions are roughly equivalent in resins, while exothermic reactions dominate in asphaltenes. During this process, the mass losses of saturates and resins are 2.1% and 0.7%, respectively, but the masses of aromatics and asphaltenes increase by 2.0% and 5.2%, respectively [22,23].

The relationship between SARA and the performance of asphalt is crucial because it defines the rheological (flow) properties, durability, and overall performance of asphalt binders under various environmental and loading conditions. Asphalt must provide structural strength while maintaining enough flexibility to resist cracking under stress. A proper balance between SARA ensures that the asphalt binder performs well under heavy loads, temperature variations, and aging processes. By understanding and optimizing the SARA balance, manufacturers can produce binders tailored to specific performance needs (e.g., heavy traffic, extreme weather) and better control over asphalt chemistry improves durability and reduces cracking, rutting, and aging, ultimately extending road service life. Also, optimized binders minimize maintenance and rehabilitation costs, reducing long-term expenditures for governments and construction companies. The studies mentioned above highlight the significant impact of SARA on the rheological properties of asphalt binders. However, most existing research primarily provides a qualitative description of the relationship between asphalt SARA and factors such as ductility, modulus, and aging, with little quantitative data on the relationship between asphalt components and mechanical properties. Furthermore, research on predicting asphalt performance based

on SARA components is sparse, indicating that the composition–structure–mechanics relationships of asphalt binders are not well understood. Currently, a major challenge for many researchers is accurately describing the relationship between asphalt components and performance, and reliably predicting performance based on SARA. In this study, SARA were obtained from 36 asphalt binders using a thin-layer chromatography with flame ionization detection (TLC-FID) analyzer, and their temperature- and frequency-dependent properties were measured by conducting frequency sweeps at different temperatures. The relationship between SARA, heavy components, colloidal instability index, complex modulus, and phase angle were analyzed. To quantitatively describe the relationship between asphalt components and mechanical properties, quadratic polynomial models and non-linear SVMs with sigmoid and RBF (Gaussian) kernels were employed to predict the complex modulus and phase angle master curve of asphalt binders based on SARA, and then reliability of these prediction models was evaluated.

2. Non-Linear Support Vector Machine

The theory of the support vector machine (SVM) originated from the field of data classification. When neural networks address linearly separable problems, the process typically involves generating a hyperplane randomly and adjusting it until the points of different categories in the training set are on opposite sides. However, this method does not ensure that the hyperplane is centrally located between the categories, which is crucial for the fault tolerance of data classification. Vapnik [24] ingeniously solved this issue with the introduction of the SVM. The core principle of the SVM is to identify the optimal linear hyperplane in the feature space that maximizes the separation of the two target classes. For both linearly separable and non-separable data, this is converted into quadratic programming (QP) to achieve a unique solution point (Figure 1). This method is effective only for linear sample sets. However, many sample sets are not linearly separable, and the use of the SVM in such cases may lead to significant risks due to its limitations. To address this, the SVM employs a linear function in a high-dimensional feature space by mapping the input vector to this space through non-linear functions, and then constructing an optimal hyperplane in this high-dimensional feature space (Non-Linear SVM, Figure 2). With the correct mapping function, most non-linearly separable problems in the input space can be transformed into linear classifications in high-dimensional feature space [25].

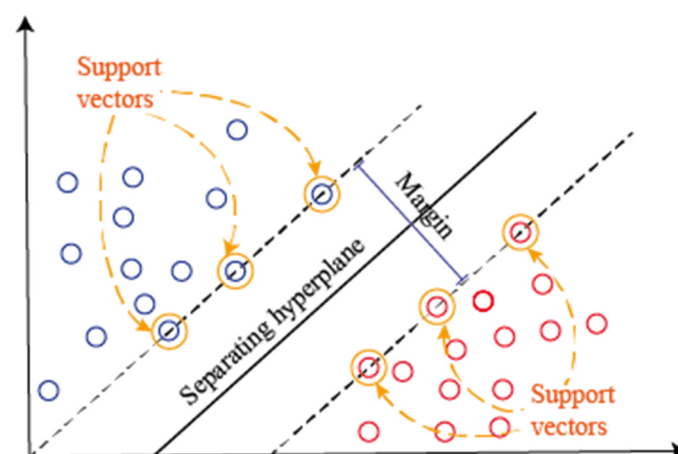


Figure 1. The optimal linear hyperplane.

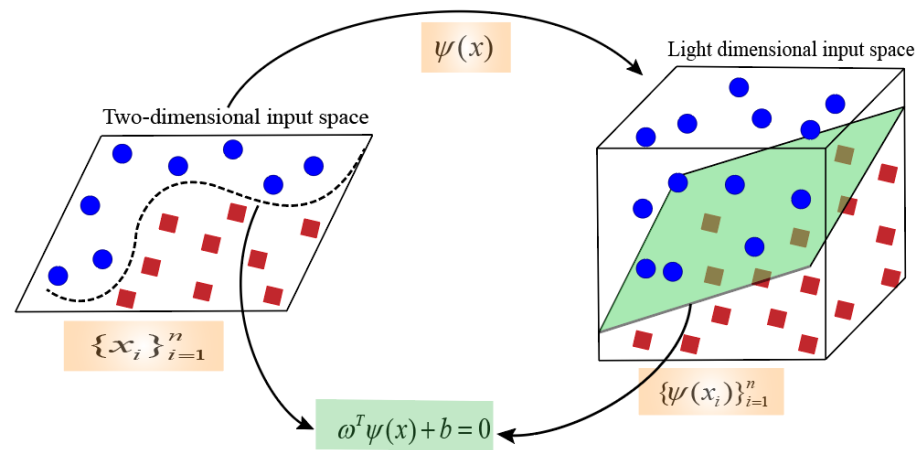


Figure 2. The non-linearly separable problem.

Recently, the SVM and non-linear SVM have been employed extensively across various scientific fields, including predicting the compressive strength and properties of fresh high-volume fly ash self-compacting concrete [26], petroleum reservoir properties [27], classification of nailfold capillary images in patients [28], soil total nitrogen, organic carbon, and moisture content [29]. One of the notable advantages of the SVM method is that, unlike neural networks which often settle at local optima, this technique is governed by a convex optimization problem. Additionally, unlike many other machine learning models that require large datasets to generalize well, SVMs are particularly effective with small to medium-sized datasets due to their reliance on support vectors. Support vectors are the critical data points that define the decision boundary, rather than using all data points, which allows SVMs to avoid overfitting when there are limited data. This achieves accurate and reliable predictions, provided the data are representative and well pre-processed. These benefits render the SVM superior to other artificial intelligence methods.

The non-linear SVM utilizes a specifically defined kernel function to address non-linear regression challenges. Commonly used kernels include the d-order polynomial kernel and the RBF (Gaussian) kernel, among others.

The d-order polynomial kernel is referred to as Function 1, while the support vector machine, functioning as a d-order polynomial classifier, is termed Function 2. Here, d is a parameter determined by the user, making the d-order polynomial kernel a global kernel [25].

$$K(x_i \cdot x) = [(x \cdot x_i) + \gamma]^d \tag{1}$$

$$f(x) = \text{sgn} \left\{ \sum_{i=1}^l y_i a_i [(x \cdot x_i) + \gamma]^d + b \right\} \tag{2}$$

The RBF (Gaussian) kernel is referred to as Function 3, and the support vector machine employing this kernel is classified as Function 4 [25].

$$K(x_i \cdot x) = \exp(-\gamma \|x - x_i\|^2) \tag{3}$$

$$f(x) = \text{sgn} \left\{ \sum_{i=1}^l y_i a_i \exp(-\gamma \|x - x_i\|^2) + b \right\} \tag{4}$$

The sigmoid kernel is defined as Function 5, and the corresponding support vector machine operates as a perceptron with hidden layers, where the number of nodes in each hidden layer is automatically determined by the algorithm [25].

$$K(x_i \cdot x) = \tanh[\gamma(x - x_i) + c] \tag{5}$$

In this paper, the d-order polynomial kernel, the RBF (Gaussian) kernel, and the sigmoid kernel have been utilized to predict the complex modulus of various asphalt binders. The performance of the proposed models is evaluated using the root-mean squared error (RMSE) [25].

$$RMSE = \sqrt{\frac{1}{n} \sum_{i=1}^n (t_i - o_i)^2} \quad (6)$$

3. Material and Experiment

3.1. Obtaining Asphalt SARA Properties

To predict the complex modulus and phase angle of asphalt binder using SARA analysis, 36 distinct types of asphalt binders were selected. The SARA properties of these binders were determined through thin-layer chromatography with flame ionization detection (TLC-FID), a technique commonly employed for analyzing components in crude oil, heavy oil, residual oil, wax, and lubricating oil asphalt. The detailed testing steps and analysis methods are described in reference [30]. The process is carried out through the following specific steps:

- (1) Separation of Saturates, Aromatics, Resins, and Asphaltenes: A 0.3 g sample of asphalt is dissolved in 30 mL of n-heptane, with gentle swirling until complete dissolution. A 1 mL aliquot of the solution is then added to a packed column and allowed to soak naturally. Successive rinsing with four different solvents is performed to elute the individual components from the column, yielding solutions of saturates, aromatics, resins, and asphaltenes in sequence.
- (2) Spotting: A 0.6 mL aliquot of each of the saturates, aromatics, resins, and asphaltenes solutions is applied to the appropriate positions on a chromatographic rod. Each solution is spotted 15 times, after which the rod is dried for 5 min.
- (3) Chromatographic Analysis: The dried chromatographic rod is placed in the TLC-FID system, where it is subjected to a hydrogen flame at a constant rate. The combustion produces electrons, which are converted into electrical signals and subsequently recorded on the display.
- (4) Spectral Analysis: The mass fraction of each component—saturates, aromatics, resins, and asphaltenes—is determined by integrating the corresponding peak areas from the resulting spectra.

The SARA data for the 36 asphalt binders are presented in Table 1.

The colloidal index (Ic) of asphalt is an important parameter that reflects the stability of the colloidal system in asphalt. The Ic provides insight into the balance between SARA, especially the relationship between the dispersed phase (asphaltenes and saturate), and the stabilizing components (resins and aromatics). The Ic helps evaluate the stability of the asphalt binder. Ic represents the ratio of the sum of asphaltenes and saturate to the sum of resins and aromatics. The proportion of heavy component (HC) in asphalt refers to the relative content of its weight components, primarily asphaltenes and resins. These heavy fractions significantly influence the physical and mechanical properties of asphalt, such as stiffness, viscosity, and aging resistance. A high proportion of heavy component increases stiffness but reduces flexibility. A low proportion improves flexibility but may reduce the binder's ability to resist permanent deformation and rutting. Therefore, this study uses the test results of the four asphalt components to calculate the colloidal index and the proportion of heavy fractions, analyzing the effect of the colloidal index and heavy fraction ratio on the dynamic mechanical properties of asphalt.

Table 1. The SARA of 36 asphalt binders obtained by TLC-FID.

| Asphalt Binder | Asphaltenes | Resins | Aromatics | Saturates |
|----------------|-------------|--------|-----------|-----------|
| 1 | 5.82 | 37.60 | 34.11 | 22.48 |
| 2 | 7.60 | 39.96 | 33.26 | 19.19 |
| 3 | 11.34 | 50.39 | 26.20 | 12.06 |
| 4 | 8.06 | 40.83 | 36.10 | 15.01 |
| 5 | 11.82 | 43.30 | 30.92 | 14.96 |
| 6 | 14.00 | 47.08 | 24.96 | 13.96 |
| 7 | 11.82 | 43.30 | 34.92 | 9.96 |
| 8 | 12.73 | 43.87 | 26.40 | 17.01 |
| 9 | 17.14 | 43.50 | 26.30 | 13.06 |
| 10 | 3.80 | 37.88 | 13.33 | 44.99 |
| 11 | 3.30 | 52.88 | 12.73 | 31.09 |
| 12 | 2.37 | 55.31 | 11.49 | 30.83 |
| 13 | 3.75 | 42.95 | 22.71 | 30.59 |
| 14 | 3.99 | 43.60 | 23.95 | 28.46 |
| 15 | 2.98 | 56.21 | 13.77 | 27.04 |
| 16 | 4.55 | 46.72 | 20.91 | 27.59 |
| 17 | 4.92 | 50.60 | 18.95 | 25.46 |
| 18 | 5.30 | 59.31 | 15.77 | 20.04 |
| 19 | 3.33 | 50.14 | 23.75 | 22.78 |
| 20 | 3.44 | 54.41 | 18.81 | 23.34 |
| 21 | 4.34 | 57.89 | 16.88 | 20.88 |
| 22 | 8.32 | 30.76 | 46.66 | 14.26 |
| 23 | 19.05 | 34.21 | 35.88 | 10.86 |
| 24 | 11.51 | 36.03 | 36.96 | 15.50 |
| 25 | 4.14 | 39.89 | 25.46 | 30.60 |
| 26 | 4.57 | 46.87 | 17.24 | 31.32 |
| 27 | 4.83 | 49.39 | 13.41 | 32.37 |
| 28 | 4.74 | 20.67 | 54.26 | 20.36 |
| 29 | 7.31 | 27.05 | 47.98 | 17.56 |
| 30 | 6.59 | 42.31 | 39.36 | 11.80 |
| 31 | 7.07 | 41.10 | 39.02 | 12.82 |
| 32 | 10.79 | 39.70 | 37.53 | 11.98 |
| 33 | 14.51 | 45.61 | 27.51 | 12.38 |
| 34 | 6.21 | 31.97 | 46.65 | 15.16 |
| 35 | 9.06 | 39.83 | 36.10 | 15.01 |
| 36 | 11.18 | 48.49 | 26.64 | 13.69 |

3.2. The Complex Modulus and Phase Angle of Asphalt

The complex modulus and phase angle of asphalt binders were measured using an AR2000 dynamic shear rheometer (DSR) manufactured by TA Corporation (Singapore). Initially, linear amplitude sweep (LAS) tests were conducted on the asphalt binders to ensure the applied shear strain remained within the linear viscoelastic interval. Subsequently, a temperature–frequency sweep was performed to determine the complex modulus and phase angle of various asphalt binders at temperatures ranging from 20 °C to 70 °C and frequencies from 0.1 to 100 Hz. Each asphalt binder was tested in three replicates. The construction of the complex modulus and phase angle master curve was based on the least squares function of Microsoft Excel. The complex modulus and phase angle of 36 asphalt binders at three different frequencies are displayed in Table 2.

Table 2. The complex modulus and phase angle of 36 asphalt binders at three different frequencies.

| Asphalt Binder | High Frequency 1000 Hz | | Medium Frequency 10 Hz | | Low Frequency 0.001 Hz | |
|----------------|---------------------------|-----------------|---------------------------|-----------------|---------------------------|-----------------|
| | G*/MPa | $\delta/^\circ$ | G*/Pa | $\delta/^\circ$ | G*/Pa | $\delta/^\circ$ |
| 1 | 12,153,900 | 52.59 | 136,842 | 77.56 | 68.9116 | 83.66 |
| 2 | 22,132,700 | 44.40 | 277,622 | 70.47 | 244.471 | 83.05 |
| 3 | 35,882,600 | 36.76 | 1,292,990 | 57.96 | 853.304 | 84.42 |
| 4 | 14,140,100 | 49.72 | 202,373 | 75.84 | 113.283 | 86.38 |
| 5 | 29,654,100 | 42.36 | 432,385 | 68.53 | 244.471 | 83.05 |
| 6 | 42,821,600 | 36.17 | 1,055,650 | 61.04 | 956.679 | 83.62 |
| 7 | 25,577,100 | 44.45 | 423,659 | 72.91 | 198.272 | 86.31 |
| 8 | 45,880,000 | 39.31 | 584,782 | 67.19 | 332.298 | 87.11 |
| 9 | 50,137,900 | 32.15 | 1,450,670 | 56.77 | 198.272 | 86.31 |
| 10 | 7,140,780 | 59.22 | 75,939.9 | 75.86 | 68.0887 | 83.41 |
| 11 | 8,243,620 | 56.20 | 133,607 | 71.04 | 147.93 | 83.54 |
| 12 | 13,505,900 | 49.11 | 262,270 | 63.91 | 68.0887 | 83.41 |
| 13 | 11,211,000 | 55.56 | 137,179 | 74.15 | 118.895 | 83.10 |
| 14 | 13,439,600 | 52.11 | 182,702 | 69.11 | 219.238 | 84.88 |
| 15 | 21,567,800 | 49.63 | 365,054 | 54.93 | 439.621 | 82.17 |
| 16 | 10,230,400 | 53.27 | 179,856 | 73.62 | 174.351 | 85.61 |
| 17 | 19,541,600 | 46.35 | 278,463 | 69.83 | 237.870 | 83.55 |
| 18 | 30,234,800 | 42.69 | 432,670 | 61.37 | 539.773 | 83.59 |
| 19 | 9,635,470 | 52.23 | 123,226 | 75.66 | 76.5012 | 86.37 |
| 20 | 16,329,100 | 46.63 | 279,415 | 70.11 | 187.791 | 84.46 |
| 21 | 28,826,400 | 38.43 | 609,089 | 60.59 | 716.599 | 83.57 |
| 22 | 7,790,010 | 53.99 | 107,880 | 76.06 | 73.4251 | 84.16 |
| 23 | 12,362,200 | 48.46 | 235,566 | 70.37 | 157.201 | 84.89 |
| 24 | 32,252,100 | 38.60 | 597,492 | 60.76 | 693.457 | 83.32 |
| 25 | 2,981,530 | 47.10 | 90,249.4 | 59.67 | 111.437 | 76.88 |
| 26 | 4,859,010 | 45.10 | 224,960 | 50.34 | 151.374 | 75.21 |
| 27 | 10,297,600 | 32.28 | 1,029,875 | 46.27 | 1241.64 | 70.88 |
| 28 | 13,650,500 | 55.09 | 147,156 | 77.74 | 77.9307 | 80.41 |
| 29 | 14,262,400 | 49.10 | 203,440 | 72.11 | 166.515 | 86.55 |
| 30 | 28,648,000 | 43.43 | 747,156 | 77.74 | 453.370 | 84.93 |
| 31 | 21,946,300 | 46.23 | 186,655 | 74.64 | 146.431 | 84.48 |
| 32 | 34,475,700 | 41.08 | 283,855 | 70.85 | 225.771 | 86.60 |
| 33 | 42,657,900 | 36.32 | 944,482 | 59.38 | 1106.84 | 83.96 |
| 34 | 9,370,620 | 47.86 | 95,010.3 | 75.28 | 73.5107 | 79.66 |
| 35 | 20,055,600 | 49.63 | 225,000 | 69.17 | 160.541 | 83.71 |
| 36 | 25,130,600 | 38.64 | 693,841 | 56.39 | 1228.19 | 81.14 |

4. Result and Discussion

4.1. Relation Between the Single Component, Complex Modulus, and Phase Angel of Asphalt

4.1.1. Relation Between the Single Component, Complex Modulus, and Phase Angel of Asphalt at Low Frequency

To fully comprehend the impact of SARS on the rheological properties of asphalt binders—specifically complex modulus and phase angle at varying temperatures—we selected three different reduced frequencies from the complex modulus and phase angle master curves: 0.001 Hz, 10 Hz, and 1000 Hz. Low frequency (0.001 Hz) is representative of very slow loading or long-term conditions, which are relevant for simulating the behavior of asphalt binders under low-stress, long-term loading situations, such as those encountered in pavement design and analysis of aging or fatigue-related issues. Intermediate frequency (10 Hz) corresponds to typical traffic loading frequencies, which are commonly observed in real-world conditions where traffic loads are applied at moderate speeds. It is often used

in studies to simulate the dynamic response of asphalt under normal service conditions. High frequency (1000 Hz) is used to simulate fast loading conditions that may occur during high-speed traffic or in laboratory settings where short-term, high-rate stresses are applied. It is also relevant for assessing the viscoelastic behavior of asphalt binders under rapidly changing conditions. These frequencies were selected to cover a broad range of practical loading scenarios, thus enhancing the relevance and applicability of our findings to real-world conditions in asphalt pavement performance analysis.

It was observed that the SARA contents exhibit non-linear influence patterns on the complex modulus and phase angle of asphalt at low frequencies (0.001 Hz), as shown in Figure 3. The presence of asphaltenes, resins, aromatics, and saturates significantly affects the rheological properties at low frequencies, with no clear correlation between the SARA contents and either complex modulus or phase angle. These complex interactions are challenging to describe precisely with mathematical formulas and are difficult to determine using traditional mathematical methods such as linear equations. However, a notable relationship exists between the ratio of heavy components and both the complex modulus and phase angle; specifically, an increase in the ratio of heavy components leads to a significant increase in complex modulus and a decrease in phase angle. Similarly, like the relationship between SARA components and rheological properties, the colloidal instability index also shows no specific correlation with the rheological properties of asphalt binders.

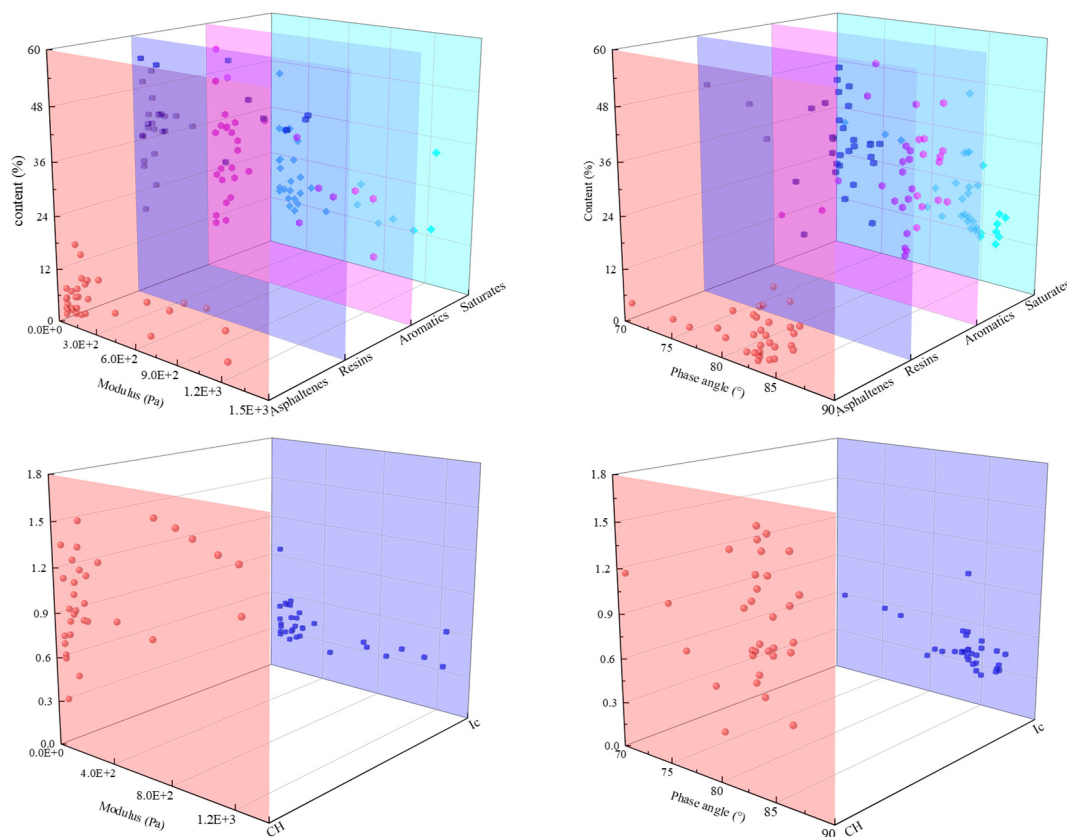


Figure 3. Relationship between the SARA, HC, Ic, and the complex modulus and phase angle of asphalt binder at low frequency.

4.1.2. Relation Between the Single Component and Complex Modulus and Phase Angel of Asphalt at Medium Frequency

The relationships between the SARA, HC, Ic, and the complex modulus, together with the phase angle of asphalt at medium frequency (10 Hz), are illustrated in Figure 4. Although there appears to be no distinct correlation between the content of asphaltenes, resins,

and aromatics and the complex modulus of asphalt at medium frequency, the complex modulus decreases as the saturates increase. Furthermore, the relationship between the SARA components of asphalt and its phase angle is complex, with no evident correlation between them. Regarding the comprehensive indicators of asphalt such as HC and Ic, it is evident that the complex modulus increases and the phase angle decreases with an increase in HC. However, the relationships between Ic, the complex modulus, and the phase angle remain ambiguous.

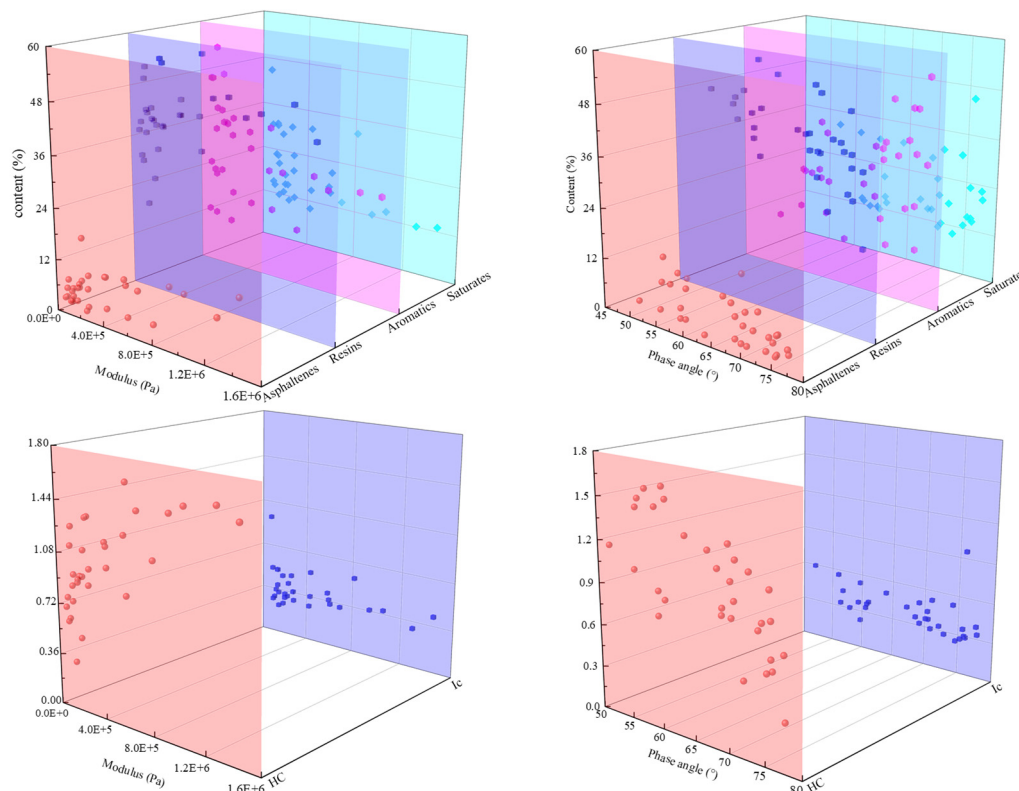


Figure 4. Relation between the SARA, HC, Ic, and the complex modulus and phase angle at medium frequency of asphalt binder.

4.1.3. Relation Between the Single Component and Complex Modulus and Phase Angel of Asphalt at High Frequency

The relationships between SARA, HC, Ic, and the complex modulus, together with the phase angle of asphalt at high frequency (1000 Hz), are depicted in Figure 5. It appears there is no clear relationship between the contents of asphaltenes, resins, and aromatics; however, the complex modulus decreases with an increase in saturates. The relationship between the SARA components of asphalt and its phase angle is complex, and SARA shows no obvious correlation with the phase angle at high frequency, similar to its behavior at low and medium frequencies. For the comprehensive indicators of asphalt such as HC and Ic, it is evident that the complex modulus increases and the phase angle decreases with HC, but the relationships between Ic, the complex modulus, and the phase angle remain unclear.

To summarize, despite the significant influence of SARA components on the rheological properties of asphalt, the complex interactions between these components, as well as the influence of external factors such as temperature and frequency, complicate the establishment of clear linear correlations. The SARA fractions—saturates, aromatics, resins, and asphaltenes—interact in non-linear and sometimes synergistic ways, which can obscure direct relationships with the complex modulus and phase angle. Additionally, the rheological behavior of asphalt binders is highly sensitive to temperature and frequency,

with these factors modulating the viscoelastic properties in ways that cannot always be captured by simple linear models. Consequently, while the individual SARA components play a crucial role in determining the overall mechanical performance, their effects are often overshadowed by these dynamic and multi-factorial interactions. Therefore, regarding the research subjects in this study—the SARA of the 36 types of asphalt binders, which cover nearly all main types of asphalt binders in asphalt pavement construction—the most significant indicators of asphalt binders show no specific relationship with the content of asphaltenes, resins, or aromatics, or the colloidal index I_c . It is only confirmed that the complex modulus increases as saturates decrease and heavy components increase. The remaining three components are interrelated and jointly influence the complex modulus and phase angle of asphalt binders by forming a colloidal structure. This suggests that the impact of SARA components on the complex modulus and phase angle is intricate and cannot be simplified into simple mathematical expressions. Alternative methods should be explored to study the rheology of asphalt from the perspective of SARA components.

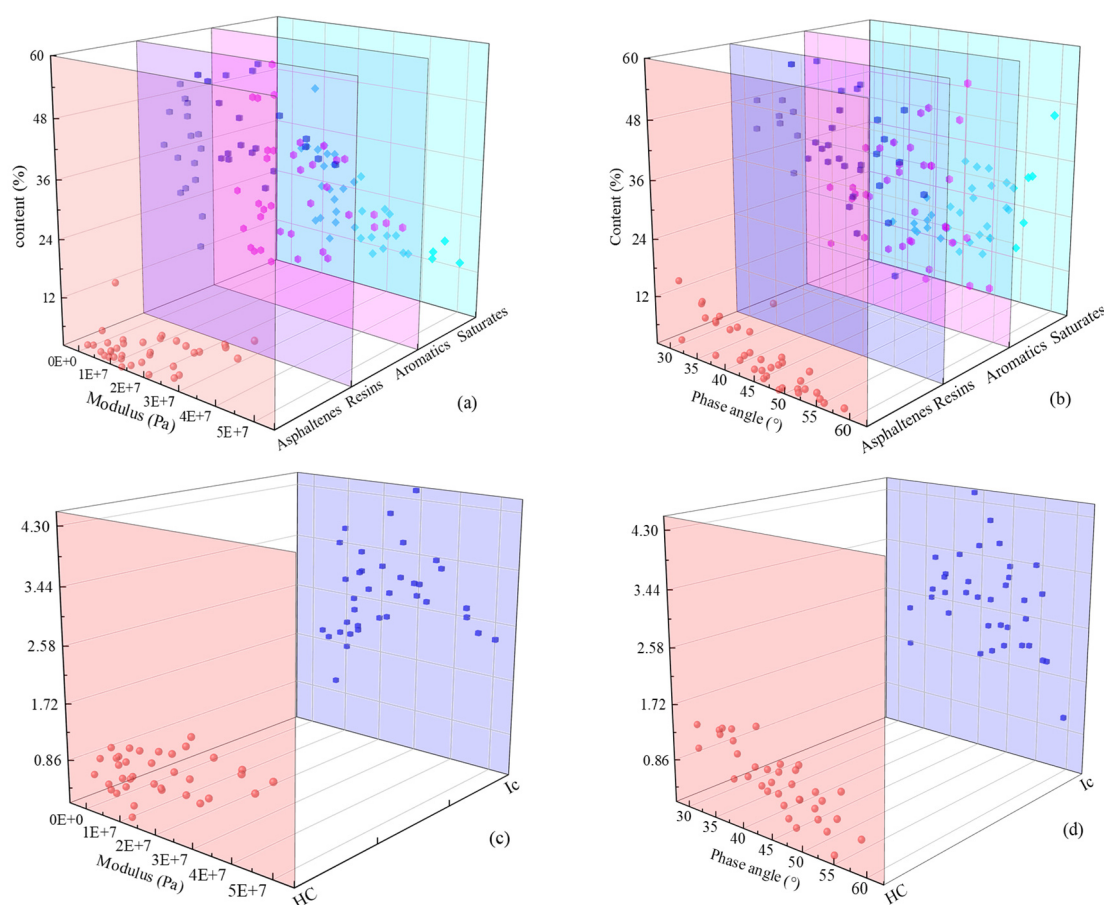


Figure 5. Relationship between the SARA contents, HC, I_c , and the complex modulus and phase angle of asphalt binder at high frequency. Relationship at high frequency: (a) the SARA contents and the complex modulus; (b) the SARA contents and phase angle of asphalt binder; (c) the HC and the complex modulus; (d) the HC and phase angle of asphalt binder.

4.2. Predicting the Complex Modulus and Phase Angle and Building the Master Curve

4.2.1. Predicting the Complex Modulus and Phase Angle Using the Quadratic Polynomial and Non-Linear SVM

The quadratic polynomial and non-linear SVM with both the sigmoid kernel and the RBF (Gaussian) kernel were utilized to predict the complex modulus and phase angle of asphalt binders based on SARA data, HC, and I_c . Components of asphalt, such as

asphaltenes, resins, aromatics, saturates, heavy components, and the colloidal index, were used as input vectors, and output vectors were derived from experimental results. The performance of the three models in predicting the complex modulus and phase angle is illustrated in Figures 6–8. The accuracy of these predictions was assessed using the correlation coefficient (R^2) and the root-mean squared error (RMSE) in Table 3. The prediction results varied significantly among the models, with RMSE values for the RBF (Gaussian) kernel at 2.6725, 3.5721, and 2.396 for the complex modulus, and 12.1947, 8.2980, and 4.3571 for the phase angle at low, medium, and high frequencies, respectively. For the quadratic polynomial, the RMSE values were 27.9251, 12.3741, and 5.7612 for the complex modulus, and 100.5855, 89.1380, and 7.6577 for the phase angle at the same frequencies. The RMSE values for the sigmoid kernel were 6.8162, 25.7219, and 8.1068 for the complex modulus, and 15.9452, 25.7219, and 19.6127 for the phase angle, respectively. The results demonstrate that the RBF kernel outperforms the quadratic polynomial and non-linear SVM with the sigmoid kernel, indicating its efficacy in predicting the complex modulus of asphalt binders subjected to different frequencies. Additionally, the prediction accuracy for all three models improved with decreasing frequency. The higher accuracy of the RBF kernel in the SVM models can be attributed to its high effectiveness in capturing non-linear relationships in data by mapping the input features into a higher dimensional space. This allows it to model complex patterns that are often present in real-world data, such as the rheological properties of asphalt binders. Also, RBF kernel-based models generally exhibit better generalization compared to other kernels. Its ability to create complex decision boundaries without overfitting makes it more robust and capable of handling noisy or high-dimensional data.

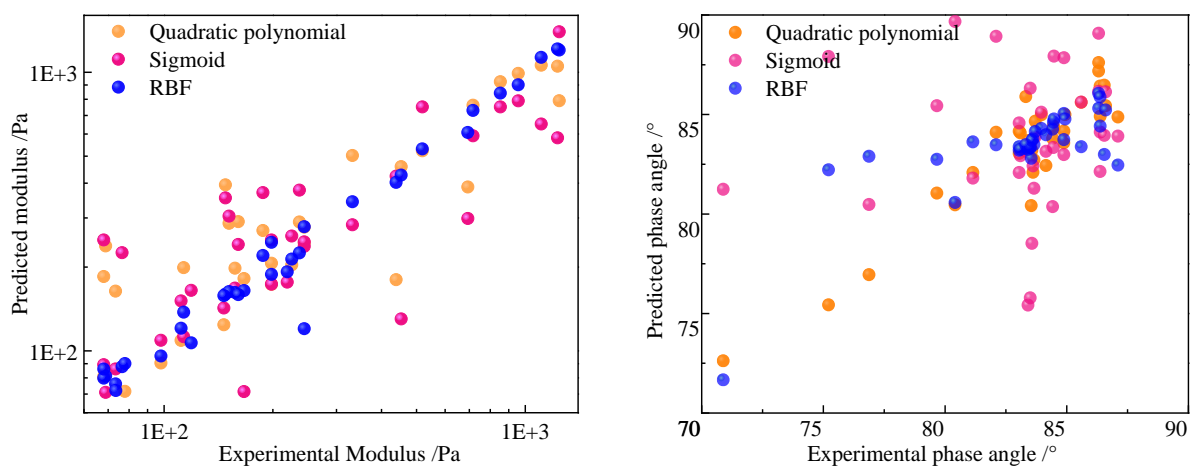


Figure 6. Prediction of the complex modulus and phase angle of asphalt at low frequency using the quadratic polynomial and the SVM with different kernel functions.

However, the RMSE values for predicting phase angle remained relatively high at low frequencies, suggesting that while the non-linear SVM with the RBF kernel is effective for predicting the complex modulus, it is less suitable for predicting the phase angle at low frequencies. Furthermore, the correlation coefficient, R^2 , also confirms that the non-linear SVM with the RBF kernel performs better than the quadratic polynomial and the non-linear SVM with the sigmoid kernel.

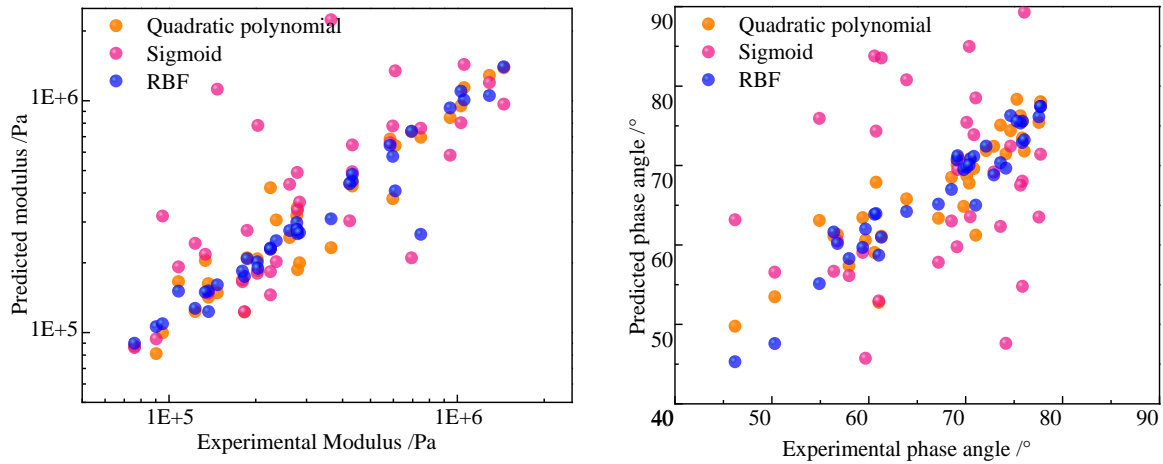


Figure 7. Prediction of the complex modulus and phase angle of asphalt at medium frequency by quadratic polynomial and the SVM with different kernel functions.

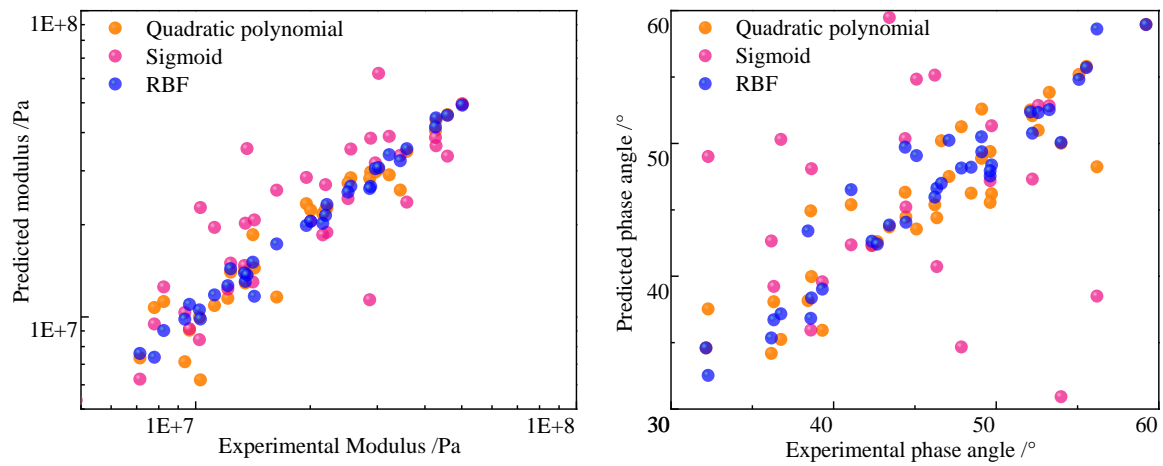


Figure 8. Prediction of the complex modulus and phase angle of asphalt at high frequency by quadratic polynomial and the SVM with different kernel functions.

Table 3. Statistical results of the quadratic polynomial and SVM models trained on collected data.

| Frequency /Hz | Experimental Test | Prediction Methods | Statistical Parameters Results | |
|---------------|-------------------|--------------------|--------------------------------|----------|
| | | | R ² | RMSE |
| 0.001 | Complex modulus | Polynomial | 0.4651 | 27.9251 |
| | | Sigmoid | 0.3567 | 6.8162 |
| | | RBF | 0.9661 | 2.6725 |
| | Phase angle | Polynomial | 0.2019 | 100.5855 |
| | | Sigmoid | 0.2523 | 15.9452 |
| | | RBF | 0.8772 | 12.1947 |
| 10 | Complex modulus | Polynomial | 0.8260 | 12.3741 |
| | | Sigmoid | 0.3821 | 25.7219 |
| | | RBF | 0.9458 | 3.5721 |
| | Phase angle | Polynomial | 0.5050 | 89.1380 |
| | | Sigmoid | 0.2886 | 11.6129 |
| | | RBF | 0.8236 | 8.2980 |
| 1000 | Complex modulus | Polynomial | 0.7461 | 5.7612 |
| | | Sigmoid | 0.5273 | 8.1068 |
| | | RBF | 0.9785 | 2.3961 |
| | Phase angle | Polynomial | 0.2371 | 7.6577 |
| | | Sigmoid | 0.2112 | 19.6127 |
| | | RBF | 0.8569 | 4.3571 |

4.2.2. Validation of the Non-Linear SVM of the RBF (Gaussian) Kernel

To validate the non-linear SVM with the RBF kernel for predicting the complex modulus and phase angle of asphalt binders at various frequencies, an experimental program was established, and the non-linear SVM of the RBF kernel was tested. Three types of asphalt binders, characterized by their SARA, HC, and Ic values, as shown in Table 4, were selected. The complex modulus and phase angle of the asphalt binders were determined through temperature–frequency sweeps, and the master curves for both were constructed using the least squares method in Microsoft Excel. To assess the accuracy of the non-linear SVM with the RBF kernel, the complex modulus and phase angle at frequencies of 0.001 Hz, 10 Hz, and 1000 Hz were calculated from the SARA, HC, and Ic of the asphalt binders. These points were then plotted and compared with the tested master curves of complex modulus and phase angle to evaluate the reliability of the non-linear SVM with the RBF kernel in predicting the complex modulus and phase angle of asphalt binders. The effectiveness of the non-linear SVM with the RBF kernel in predicting the master curves for complex modulus and phase angle of the asphalt binders can be seen in Figure 9. The results showed that the trained SVM with the RBF kernel successfully learned the relationship between input (SARA component) and output (complex modulus) vectors for different asphalt binders. The predicted complex modulus master curves closely matched the tested results, indicating that using an appropriate input vector for prediction models and finding optimum values of the kernel function using a suitable method can lead to an accurate model capable of predicting the complex modulus of asphalt binders.

Table 4. SARA, HC, and Ic of selected asphalt binders.

| Asphalt Binder | Asphaltenes | Resins | Aromatics | Saturates |
|----------------|-------------|--------|-----------|-----------|
| Sample 1 | 8.06 | 40.83 | 36.10 | 15.01 |
| Sample 2 | 17.14 | 43.50 | 26.30 | 13.06 |
| Sample 3 | 4.34 | 57.89 | 16.88 | 20.88 |

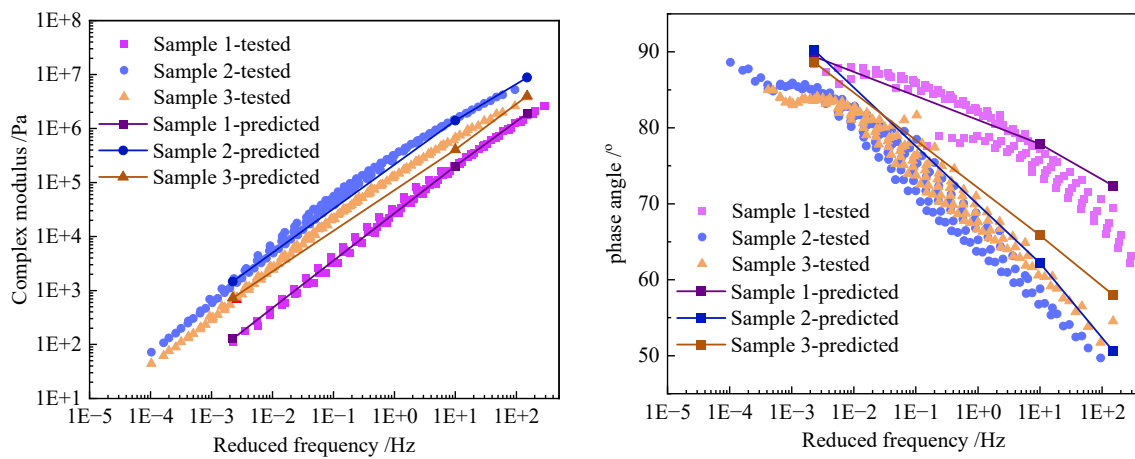


Figure 9. Validation of the SVM for prediction of the complex modulus and phase angle of asphalt binders.

However, the predicted master curves for phase angle significantly deviated from the tested results, especially at low frequencies. This suggests that the SVM with the RBF kernel is unable to accurately predict the phase angle of asphalt binders from SARA, and instead, it only approximates the trend of phase angle changes with frequency.

5. Conclusions

The aim of this research was to explore the relationships between the SARA fraction and the varying mechanical properties of asphalt binders at different temperatures and frequencies. SARA data were collected from 36 asphalt binders to examine their impact on the complex modulus and phase angle at various frequencies. Additionally, the quadratic polynomial and non-linear SVM with the sigmoid kernel and the RBF (Gaussian) kernel were employed to predict the complex modulus and phase angle of asphalt binders based on SARA, and the reliability of these prediction models was evaluated. The following conclusions can be drawn.

1. The content of asphaltenes, resins, aromatics, and saturates demonstrated the most complex effects on the rheological properties at different frequencies, with no clear correlation between SARA components and the complex modulus or phase angle. An increase in the ratio of heavy components led to a significant increase in complex modulus and a decrease in phase angle at each frequency. The colloidal instability index showed no specific relationship with the complex modulus and phase angle of asphalt binders at low, medium, or high frequency.
2. The impact of SARA on the complex modulus and phase angle is intricate and cannot be simplified through straightforward mathematical formulations. Alternative methods should be employed to study the mechanical properties of asphalt based on SARA.
3. The quadratic polynomial and non-linear SVM with both the sigmoid kernel and the RBF (Gaussian) kernel were applied to predict the complex modulus and phase angle of asphalt binders using SARA, the ratio of heavy components, and the colloidal instability index. The results indicate that the RBF kernel performs better than the quadratic polynomial and the non-linear SVM with the sigmoid kernel. Additionally, the accuracy of all three models improved as the frequency decreased. However, despite the high accuracy of the non-linear SVM with the RBF kernel in predicting complex modulus, it was not suitable for predicting the phase angle at low frequencies.
4. The validation of the non-linear SVM with the RBF kernel for predicting the complex modulus and phase angle of asphalt binders demonstrated that the trained SVM effectively learned the relationship between input (SARA component) and output (complex modulus) vectors for different asphalt binders. The predicted complex modulus master curves closely matched the tested results. However, the predicted master curves for the phase angle deviated significantly from the tested results, particularly at low frequencies. The SVM with the RBF kernel was unable to predict the phase angle of asphalt binders from SARA accurately and merely approximated the trend of phase angle changes with frequency.

Author Contributions: Conceptualization, S.S. and Y.M.; methodology, X.J.; software, D.L.; validation, X.M. and S.Q.; formal analysis, X.M.; funding acquisition, S.S. All authors have read and agreed to the published version of the manuscript.

Funding: This project was supported by Gansu Provincial Science and Technology Plan (23JRRA1375, 21JR7RA786) and Research project of Gansu Provincial Department of Transportation (2022-22, 2022-33), Lanzhou Youth Science and Technology Talent Innovation Project (2023-QN-102), China Postdoctoral Science Foundation Funded Project (Project No. 2020M683401), the Natural Science Basis Research Plan in Shaanxi Province of China (No. 2021JQ-262), the Fundamental Research Funds for the Central Universities of China (No. 300102311105).

Institutional Review Board Statement: Not applicable.

Informed Consent Statement: Not applicable.

Data Availability Statement: The data supporting the findings of this study are contained within the article.

Acknowledgments: The authors gratefully acknowledge support from Chang'an University and Scientific Observation and Research Base of Transport Industry of Long Term Performance of Highway Infrastructure in Northwest Cold and Arid Regions.

Conflicts of Interest: Author Shanglin Song was employed by the company Gansu Provincial Highway Development Group Co., Ltd. Author Xiaoqiang Jiang and Dengzhou were employed by the company Gansu Hengtong Road and Bridge Engineering Co., Ltd. The remaining authors declare that the research was conducted in the absence of any commercial or financial relationships that could be construed as a potential conflict of interest.

References

1. Weigel, S.; Stephan, D. Relationships between the chemistry and the physical properties of bitumen. *Road Mater. Pavement Des.* **2017**, *19*, 1636–1650. [[CrossRef](#)]
2. Wang, J.; Wang, T.; Hou, X.; Xiao, F. Modelling of rheological and chemical properties of asphalt binder considering SARA fraction. *Fuel* **2019**, *238*, 320–330. [[CrossRef](#)]
3. Mirwald, J.; Werkovits, S.; Camargo, I.; Maschauer, D.; Hofko, B.; Grothe, H. Understanding bitumen ageing by investigation of its polarity fractions. *Constr. Build. Mater.* **2020**, *250*, 118809. [[CrossRef](#)]
4. Yang, C.; Xie, J.; Wu, S.; Amirkhanian, S.; Zhou, X.; Ye, Q.; Yang, D.; Hu, R. Investigation of physicochemical and rheological properties of SARA components separated from bitumen. *Constr. Build. Mater.* **2020**, *235*, 117437. [[CrossRef](#)]
5. Wang, J.; Xiao, F. Rheological Properties of Derivative Fractions Composed of Aromatics, Resins, and Asphaltenes. *J. Test. Eval.* **2022**, *50*, 1572–1586. [[CrossRef](#)]
6. Xu, Y.; Zhang, E.; Shan, L. Effect of SARA on Rheological Properties of Asphalt Binders. *J. Mater. Civ. Eng.* **2019**, *31*, 04019086. [[CrossRef](#)]
7. Leite, L.F.M.; Osmari, P.H.; Aragão, F.T.S. Rheological indexes for asphalt binders considering different aging conditions: Evaluation and correlations with performance. *Constr. Build. Mater.* **2022**, *338*, 127549. [[CrossRef](#)]
8. Xiao, M.M.; Fan, L. Ultraviolet aging mechanism of asphalt molecular based on microscopic simulation. *Constr. Build. Mater.* **2022**, *319*, 126157. [[CrossRef](#)]
9. Ghasemirad, A.; Bala, N.; Hashemian, L. High-Temperature Performance Evaluation of Asphaltenes-Modified Asphalt Binders. *Molecules* **2020**, *25*, 3326. [[CrossRef](#)]
10. Wang, T.; Wang, J.; Hou, X.; Xiao, F. Effects of SARA fractions on low temperature properties of asphalt binders. *Road Mater. Pavement Des.* **2019**, *22*, 539–556. [[CrossRef](#)]
11. Hofer, K.; Mirwald, J.; Bhasin, A.; Hofko, B. Low-temperature characterization of bitumen and correlation to chemical properties. *Constr. Build. Mater.* **2023**, *366*, 130202.
12. Zhang, E.; Shan, L.; Qi, X.; Wang, X.; Fan, Y. Investigating the relationship between chemical composition and mechanical properties of asphalt binders using atomic force microscopy (AFM). *Constr. Build. Mater.* **2022**, *343*, 128001. [[CrossRef](#)]
13. Zhao, K.; Wang, Y.; Li, F. Influence of ageing conditions on the chemical property changes of asphalt binders. *Road Mater. Pavement Des.* **2019**, *22*, 653–681. [[CrossRef](#)]
14. Sun, W.; Wang, H. Molecular dynamics simulation of nano-crack formation in asphalt binder with different SARA fractions. *Mol. Simul.* **2022**, *48*, 789–800. [[CrossRef](#)]
15. Salehfard, R.; Behbahani, H.; Dalmazzo, D.; Santagata, E. Effect of colloidal instability on the rheological and fatigue properties of asphalt binders. *Constr. Build. Mater.* **2021**, *281*, 122563. [[CrossRef](#)]
16. Li, J.; Huang, X.; Zhang, Y.; Xu, M. Bitumen Colloidal and Structural Stability Characterization. *Road Mater. Pavement Des.* **2011**, *10*, 45–59. [[CrossRef](#)]
17. Guo, M.; Liang, M.; Fu, Y.; Sreeram, A.; Bhasin, A. Average molecular structure models of unaged asphalt binder fractions. *Mater. Struct.* **2021**, *54*, 173. [[CrossRef](#)]
18. Wang, P.; Dong, Z.-J.; Tan, Y.-Q.; Liu, Z.-Y. Investigating the Interactions of the Saturate, Aromatic, Resin, and Asphaltene Four Fractions in Asphalt Binders by Molecular Simulations. *Energy Fuels* **2015**, *29*, 112–121. [[CrossRef](#)]
19. Eberhardsteiner, L.; Füssl, J.; Hofko, B.; Handle, F.; Hospodka, M.; Blab, R.; Grothe, H. Micromechanical Description of Bitumen Aging Behavior. In *8th RILEM International Symposium on Testing and Characterization of Sustainable and Innovative Bituminous Materials*; Springer: Dordrecht, The Netherlands, 2016; pp. 411–421.
20. Zhang, C.; Xu, T.; Shi, H.; Wang, L. Physicochemical and pyrolysis properties of SARA fractions separated from asphalt binder. *J. Therm. Anal. Calorim.* **2015**, *122*, 241–249. [[CrossRef](#)]

21. Xia, W.; Xu, T. Thermal Characteristics, Kinetic Models, and Volatile Constituents during the Energy Conversion of Bituminous SARA Fractions in Air. *ACS Omega* **2020**, *5*, 20831–20841. [[CrossRef](#)] [[PubMed](#)]
22. Hu, Z.; Zhang, H.; Wang, S.; Xu, T. Thermal-oxidative aging mechanism of asphalt binder based on isothermal thermal analysis at the SARA level. *Constr. Build. Mater.* **2020**, *255*, 119349. [[CrossRef](#)]
23. Xia, W.; Wang, S.; Wang, H.; Xu, T. Thermal effects of asphalt SARA fractions, kinetic parameter calculation using isoconversional method and distribution models. *J. Therm. Anal. Calorim.* **2020**, *146*, 1577–1592. [[CrossRef](#)]
24. Do, T.-N. Non-linear Classification of Massive Datasets with a Parallel Algorithm of Local Support Vector Machines. In *Advanced Computational Methods for Knowledge Engineering: Proceedings of 3rd International Conference on Computer Science, Applied Mathematics and Applications-ICCSAMA 2015, Metz, France, 11–13 May 2015*; Springer: Cham, Switzerland, 2015; pp. 231–241.
25. Zhao, H.; Yao, Y.; Liu, Z. A Classification Method Based on Non-linear SVM Decision Tree. In *Proceedings of the Fourth International Conference on Fuzzy Systems and Knowledge Discovery (FSKD 2007)*, Haikou, China, 24–27 August 2007; IEEE: Piscataway, NJ, USA, 2007; pp. 635–638.
26. Azimi-Pour, M.; Eskandari-Naddaf, H.; Pakzad, A. Linear and non-linear SVM prediction for fresh properties and compressive strength of high volume fly ash self-compacting concrete. *Constr. Build. Mater.* **2020**, *230*, 117021. [[CrossRef](#)]
27. Otchere, D.A.; Ganat, T.O.A.; Gholami, R.; Ridha, S. Application of supervised machine learning paradigms in the prediction of petroleum reservoir properties: Comparative analysis of ANN and SVM models. *J. Pet. Sci. Eng.* **2021**, *200*, 108182. [[CrossRef](#)]
28. Nivedha, R.; Brinda, M.; Suma, K. Classification of Nailfold Capillary Images in Patients with Hypertension Using Non-linear SVM. In *Proceedings of the 2016 International Conference on Circuits, Controls, Communications and Computing (I4C)*, Bangalore, India, 4–6 October 2016; IEEE: Piscataway, NJ, USA, 2016; pp. 1–5.
29. Morellos, A.; Pantazi, X.-E.; Moshou, D.; Alexandridis, T.; Whetton, R.; Tziotziou, G.; Wiebensohn, J.; Bill, R.; Mouazen, A.M. Machine learning based prediction of soil total nitrogen, organic carbon and moisture content by using VIS-NIR spectroscopy. *Biosyst. Eng.* **2016**, *152*, 104–116. [[CrossRef](#)]
30. Ma, X.; Ma, X.; Wang, Z.; Song, S.; Sheng, Y. Investigation of changing SARA and fatigue properties of asphalt bitumen under ageing and analysis of their relation based upon the BP neural network. *Constr. Build. Mater.* **2023**, *394*, 132163. [[CrossRef](#)]

Disclaimer/Publisher’s Note: The statements, opinions and data contained in all publications are solely those of the individual author(s) and contributor(s) and not of MDPI and/or the editor(s). MDPI and/or the editor(s) disclaim responsibility for any injury to people or property resulting from any ideas, methods, instructions or products referred to in the content.